SAND2017-0777J

The Recommendations for Linear Measurement Techniques on the Measurements of Nonlinear System Parameters of a Joint

Scott A. Smith[1,2*], Simone Catalfamo[3], Matthew R.W. Brake[2,4], Christoph W. Schwingshackl[5], and Pascal Reuß[6]

[1] University of Maryland, Baltimore County, 1000 Hilltop Circle, Baltimore, MD 21250, USA
[2] Sandia National Laboratories[§], 1515 Eubank Blvd SE, Albuquerque, NM 87123, USA
[3] University of Stuttgart, Keplerstraße 7, 70174 Stuttgart, Germany
[4] William Marsh Rice University, 6100 Main St, Houston, TX 77005, USA
[5] Imperial College London, London SW7 2AZ, United Kingdom
[6] Daimler AG, 70546 Stuttgart, Germany

Abstract

In the study of the dynamics of nonlinear systems, experimental measurements often convolute the response of the nonlinearity of interest and the effects of the experimental setup. To reduce the influence of the experimental setup on the deduction of the parameters of the nonlinearity, the response of a mechanical joint is investigated under various experimental setups. The experiments first focus on quantifying how support structures and measurement techniques affect the natural frequency and damping of a linear system. The results indicate that support structures created from bungees have negligible influence on the system in terms of frequency and damping ratio variations. The study then focuses on the effects of the excitation technique on the response for a linear system. The findings suggest that thinner stingers should not be used, because under the high force requirements the stinger bending modes are excited adding unwanted torsional coupling. The optimal configuration for testing the linear system is then applied to a nonlinear system in order to assess the robustness of the test configuration. Finally, recommendations are made for conducting experiments on nonlinear systems using conventional/linear testing techniques.

Keywords: Bolted joints; Nonlinear vibration; Experimental setup; Measurement effects; Testing guidelines

1 Introduction

The principles of modal analysis are based on linear vibration theory [1]. This assumes that the modes are uncoupled, that natural frequencies and damping ratios are constant, and that the response is linearly proportional to the excitation. For nonlinear systems, even those that might be considered weakly nonlinear, these assumptions break down: the modes are coupled, the natural frequencies and damping ratios are amplitude dependent, the response is not proportional to the

* Corresponding Author: ssmith11@umbc.edu

§ Sandia National Laboratories is a multi-mission laboratory managed and operated by Sandia Corporation, a wholly owned subsidiary of Lockheed Martin Company, for the U. S. Department of Energy's National Nuclear Security Administration under Contract DE-AC04-94AL85000

excitation, etc. As a result, a new theory for nonlinear analysis of experiments is needed and a large amount of research effort is currently focused on developing it (e.g., Nonlinear normal modes) [2, 3]. Until said theory is developed, though, the limitations and dangers of linear methods to assess the dynamics of a nonlinear system must be better understood. This paper is a first step in that process.

Studying the response of nonlinear systems is a challenging effort. The increased effort stems from multiple stable and unstable equilibria, resulting in the measurements of the system being sensitive to excitation and initial conditions. The effort also arises from an insufficient understanding of the physics governing the nonlinearity's response. The nonlinearity often manifests itself when a small change in the constitutive model generates a large change in the response [4, 5, 6].

Because of this, experimental measurements often convolute the effects of the nonlinearity of interest with the experimental setup [7, 8]. The very act of measuring the response of a system can fundamentally change the system (much like the observer effect in quantum physics [9]). By creating a support structure or attaching a gage or other instruments to a specimen, the system is no longer the original specimen, but rather a combination of the specimen and the experimental setup. A shaker, for instance, can change the impedance of a system dramatically due to the method by which it is attached to the system. Further, a fixed boundary condition is difficult to achieve; in most cases torsional stiffness, friction, and even gaps are still present. By contrast, a free boundary condition is often accurately emulated via bungee cords or foam pads, which act as weak springs. These issues are further influenced by the test specimen itself. Attaching a five-gram accelerometer to a solid cube that weighs 50 kg will have less of an effect then attaching the same accelerometer to a highly flexible, light weight body such as an aero-shell. The effects of accelerometer mass have a larger influence in nonlinear analysis on highly flexible structures; this is from the need of high amplitudes of excitation and the potential need to measure many harmonics.

Considering these known issues, the following questions emerge:

1. What support structure will minimally affect the dynamics of a system?
2. What is the optimal manner in which to excite the system?

To address these questions, a benchmark nonlinear structure, commonly termed the Brake-Reuß Beam (BRB), containing a lap joint is used, the beam is detailed in [10] using 5/16"-24 bolts instead of M8 bolts. The beam, shown in Figure 1, is designed to have a simple geometry that contains nonlinear effects from a lap-joint. The lap-joint is an ideal system due to the effect of the nonlinearity on the transfer function (TF) [10], which is not always obvious in all systems [3, 11].

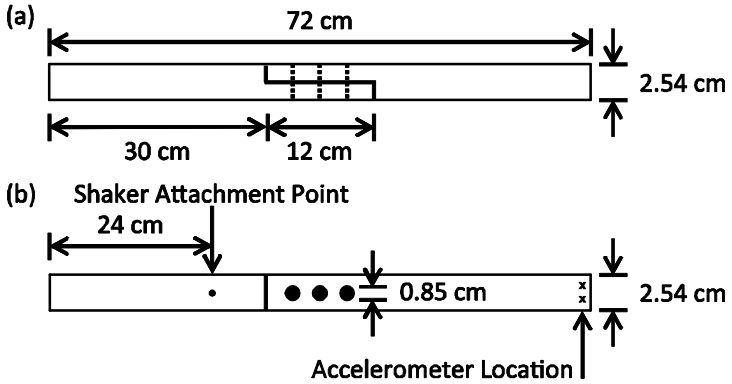

Figure 1: The Geometry of the Brake-Reuß Beam.

In this work, an analysis of a monolithic beam and the BRB is conducted. The analysis studies the effects of different loading/excitation conditions, instrumentation configurations, and boundary conditions. The experiments are conducted with either a "free-free" or "fixed-free" boundary condition. First, in Section 2, a monolithic beam with the same dimensions as the BRB is studied by using a modal hammer with different boundary and equipment setups. Next, in Section 3, the study is expanded to uncontrolled shaker signals (e.g., white noise, sweeps, etc.); and then to the study of the linear control parameters using the BRB. Finally, recommendations for the measurements of a nonlinear system with a mechanical joint are given in Section 4.

2 Effects of Experimental Setup

Isolating the effects of a lap-joint on the dynamic response of a system necessitates a linear, or as close as possible, design of the test setup; this is needed so that the nonlinearity of the joint is not convoluted with any other nonlinearities. Sources of unwanted nonlinearities are: misalignment, pre-loads, cable rattling, poor transducer mounting, etc. [12]. These unwanted nonlinearities are more likely to occur under high levels of excitation; and their effects need to be accounted. The damping added due to the test setup need to be measured and studied for any nonlinearities that maybe added into the system [13, 14].

To study the effects of the test setup, a monolithic beam is fabricated using stainless steel 304. The experimental setup, shown in Figure 2, includes the beam, two bungee cords, two PCB 356A01 Triaxial ICP Accelerometers (Accels), two PCB 356A03 Triaxial Accels used in a second experimental setup, a PCB 086C03 ICP Impact Hammer (Hammer), a Brüel & Kjær PM Vibration Exciter Type 4809 (Shaker), LMS 16 Channel Spectral Analyzer, and a modular test rig made using Newport X95 rails.

To gain an understanding of the vibration of the monolithic beam, modal analysis using the roving hammer technique [15] was performed. The mode shapes, natural frequencies, and modal damping ratios of the monolithic beam (without shaker attached) are measured with the use of 58 impact lines and two impacts per line. The natural frequencies and modal damping ratios are listed in Table 1, and the mode shapes are displayed in Figure 3. The mode numbers used in Figure 3 are those calculated using the Finite Element software Abaqus 6.10; similar values are found via other

software packages as well, such as SIERRA and Hyperworks [16]. The seventh mode (3472 Hz from analytical equations) is the first axial mode, which is not excited in the present experiment.

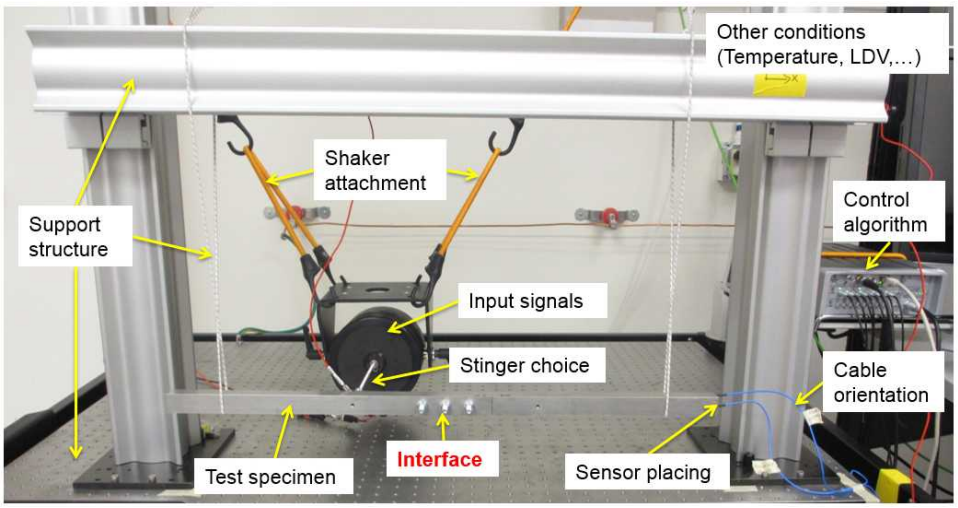

Figure 2: Basic test setup for testing the effects of boundary conditions, excitation techniques, and sensor setup.

Table 1: Modal testing results on the monolithic beam.

Mode	Frequency (Hz)	Modal Damping (%)
1st Bending	246.3	0.03
2nd Bending	674.5	0.04
3rd Bending	1308.5	0.03
1st Torsional	1965.0	0.03
4th Bending	2130.7	0.04
5th Bending	3126.8	0.04
2nd Torsional	3931.8	0.05

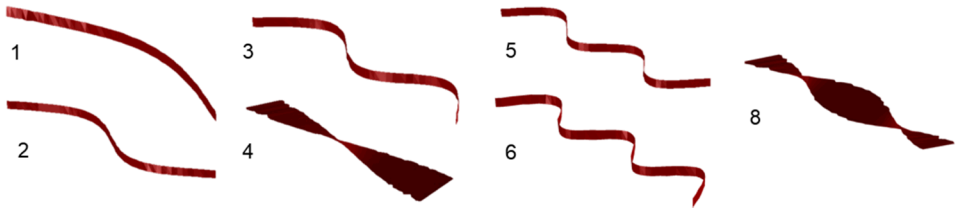

Figure 3: Mode shapes measured in modal analysis.

2.1 Experimental Setup Excited by Impact Hammer

The effects of the experimental setup are grouped into four categories: 1) impact hammer excitation effects, 2) "free-free" boundary condition approximation effects, 3) instrumentation effects, and 4) test rig effects. The various experimental setups tested in this category are listed in Table 2; with each test conducted with a metal and plastic hammer tip, and high and low impact levels.

Table 2: Experimental setups tested for nonlinear influences.

Test Number	Bungee Cord Stiffness	Bungee Cord Location	Bungee Cord Length (m)	Accelerometer Mass (gm)	Accelerometer Attachment	Hammer Mass (gm)	Accelerometer Cable Orientation
1	High	Inside	0.318	1	Glue	160	Above
2	High	Inside	0.318	1	Glue	235	Above
3	High	Outside	0.318	1	Glue	160	Above
4	High	Outside	0.165	1	Glue	160	Above
5	Low	Outside	0.318	1	Glue	160	Above
6	Low	Outside	0.318	1	Wax	160	Above
7	Low	Outside	0.318	10.5	Wax	160	Above
8	Low	Outside	0.318	1	Glue	160	Across
9	Low	Outside	0.318	1	Glue	160	Unsupported

2.1.1 Impact Hammer

Impact hammers are only in contact with a system long enough to transmit a short duration force (typically <1ms), unlike a shaker that is typically attached to a system for an entire experiment. As a result, the response due to an impact hammer excitation is often considered the "true" representation of a system. Of course, impact hammers are limited in the range, type, and duration of forces that they can transmit to a system, which make other excitation techniques more attractive for some studies. In the first set of experiments, the effects of the impact hammer tips (metal versus plastic) and mass (160gm versus 235gm) are studied for different impact levels (high versus low). The tests are summarized in Table 2 as Tests 1 and 2, and the FRFs for the hammer setups are shown in Figure 4.

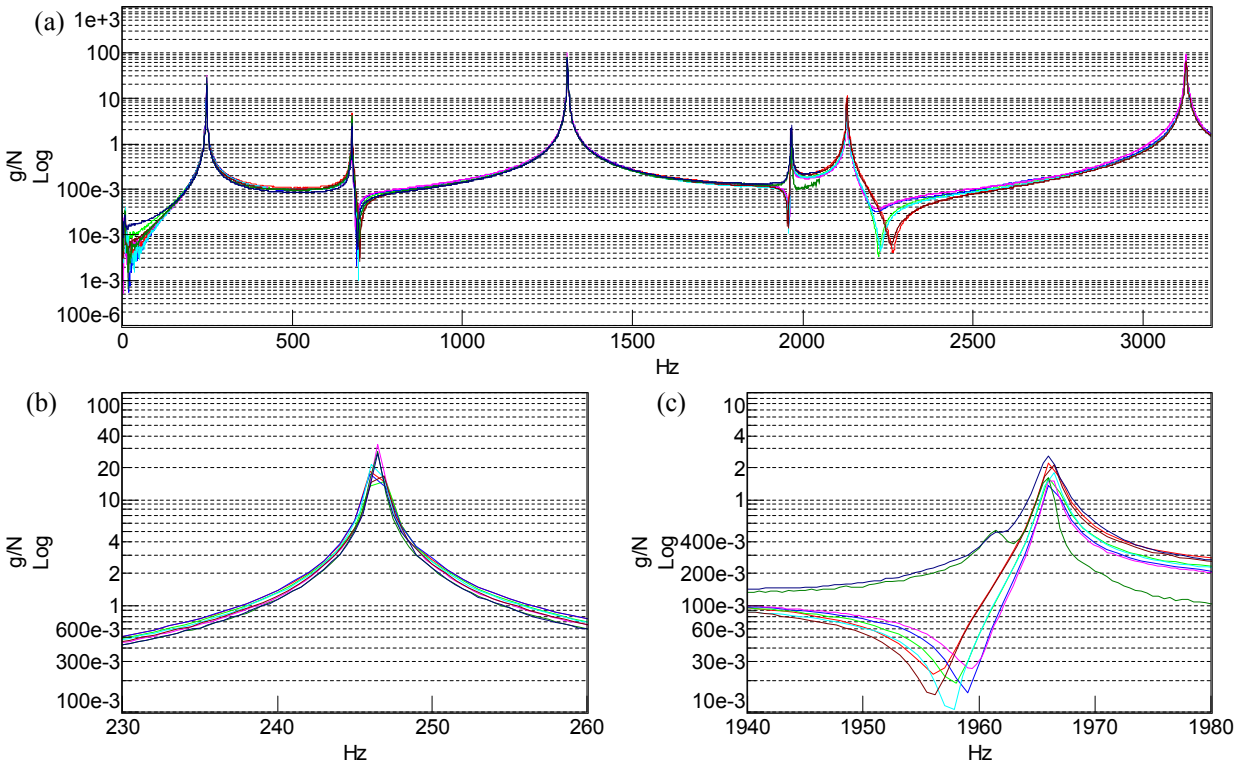

Figure 4: The FRFs of the impact hammer study (Table 2 Tests 1 and 2) for (a) the entire frequency range, (b) the first bending, and (c) first torsional mode.

The results of the tests show that the hammer tip, mass, and impact level do not have an appreciable influence on the response of the linear system, as expected. For linear systems, the response is linearly proportional to the excitation amplitude. The selection of the impact hammer tip and mass is governed by the frequency range of interest. For higher frequencies a harder tip and lighter hammer are needed. The difference in the first torsional mode could be from the impacts being in a slightly different location, which highlights the downside of using an impact hammer.

2.1.2 Support Structure

The second set of experiments consider the support structure: the length (0.318m versus 0.1651m), position (inside, 10.2cm separated centered, or outside, 5.72cm from edges of the beam) and stiffness (low ~37.8N/m, or high ~49.5N/m, which are measured) of the bungee cords used to approximate a "free" boundary condition; listed in Table 2 as Tests 1 and 3 through 5. The inside location was selected to keep the beam balanced as well as allow the edges of the beam to more freely vibration; the outside location was selected to have enough space that if the bungees slid there was room to keep the specimen suspended. The bungees are crossed to keep the specimen aligned. The FRFs for the support structure variations are shown in Figure 5.

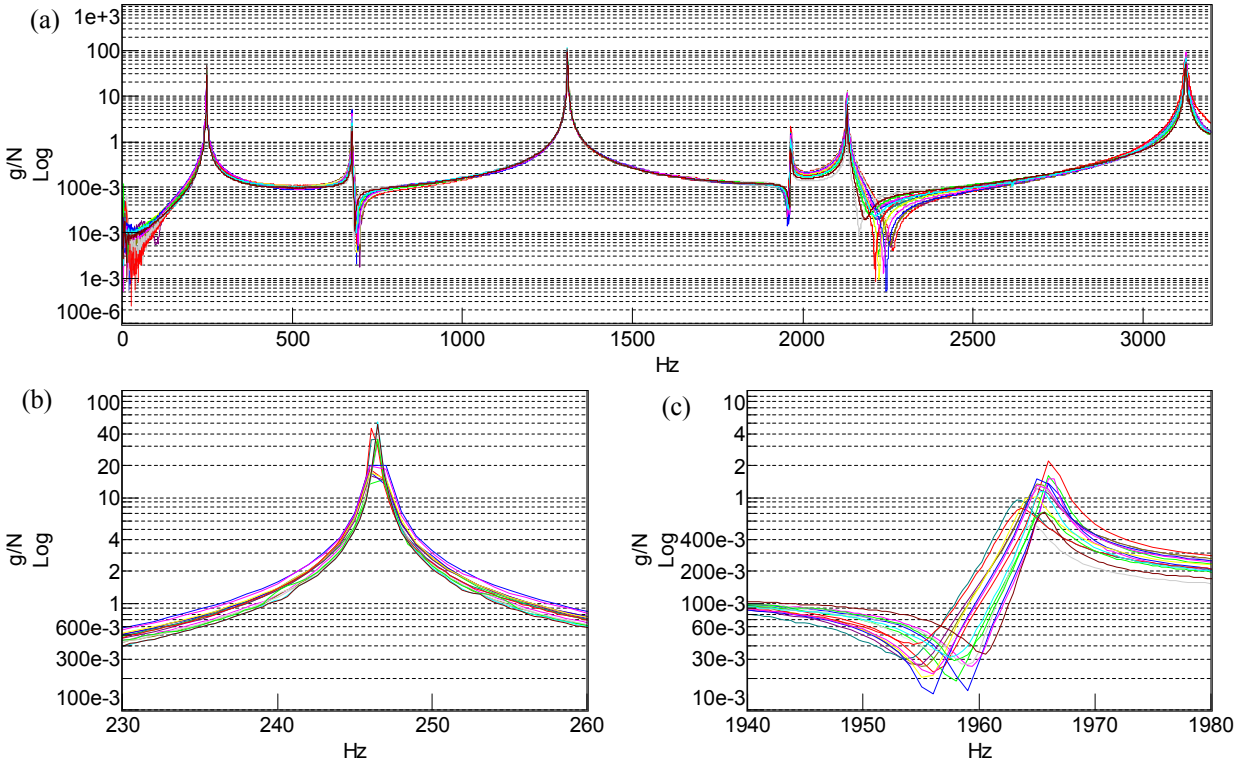

Figure 5: The FRFs of the bungee support structure testing (Table 2 Tests 1, 3, 4, and 5) for (a) the entire frequency range, (b) the first bending, and (c) first torsional mode.

The most of the modes do not show any significant nonlinearity due to the test setup, which is desirable and confirms the findings in [14]. The only nonlinearity observed occurs in the torsional modes, which are constrained by the bungee cords. Unlike the impact hammer tests, in which the natural frequencies of the torsional modes are approximately constant, the measured natural frequencies are observed to shift by 3Hz. The shift of frequencies could be happening from the bungees slipping, which leads to some friction which generates damping and softening. Previous studies have observed that the damping caused by the boundary conditions can influence lightly damped structures [17]. The torsional mode nonlinearities observed could potentially be removed by alternative suspension materials. A slight improvement can be obtained by using a hybrid bungee-fishing line support structure (hereafter referred to as the hybrid support) in which the fishing line is directly supporting the specimen. This setup is further illustrated in Figure 6, as well as a typical foam support and fishing line support. The foam support tested only supported the beam for five centimeters at each end in order to minimize the stiffness and damping that the foam might add to the system. The foam used was not the softest available, because the soft foam touched all but the top surface of the beam which would constrain the response more than a slightly stiffer foam. The response with the hybrid support, fishing line support, and foam support is compared to the response of Test 3 in Figure 7.

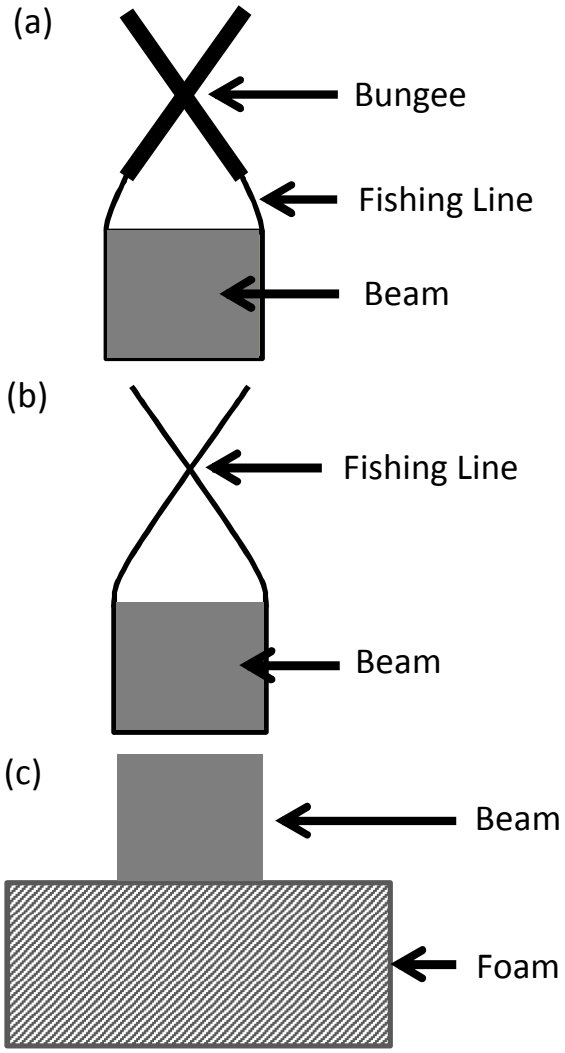

Figure 6: Alternative boundary conditions – (a) Bungee-fishing line hybrid, (b) foam supports and (c) fishing line.

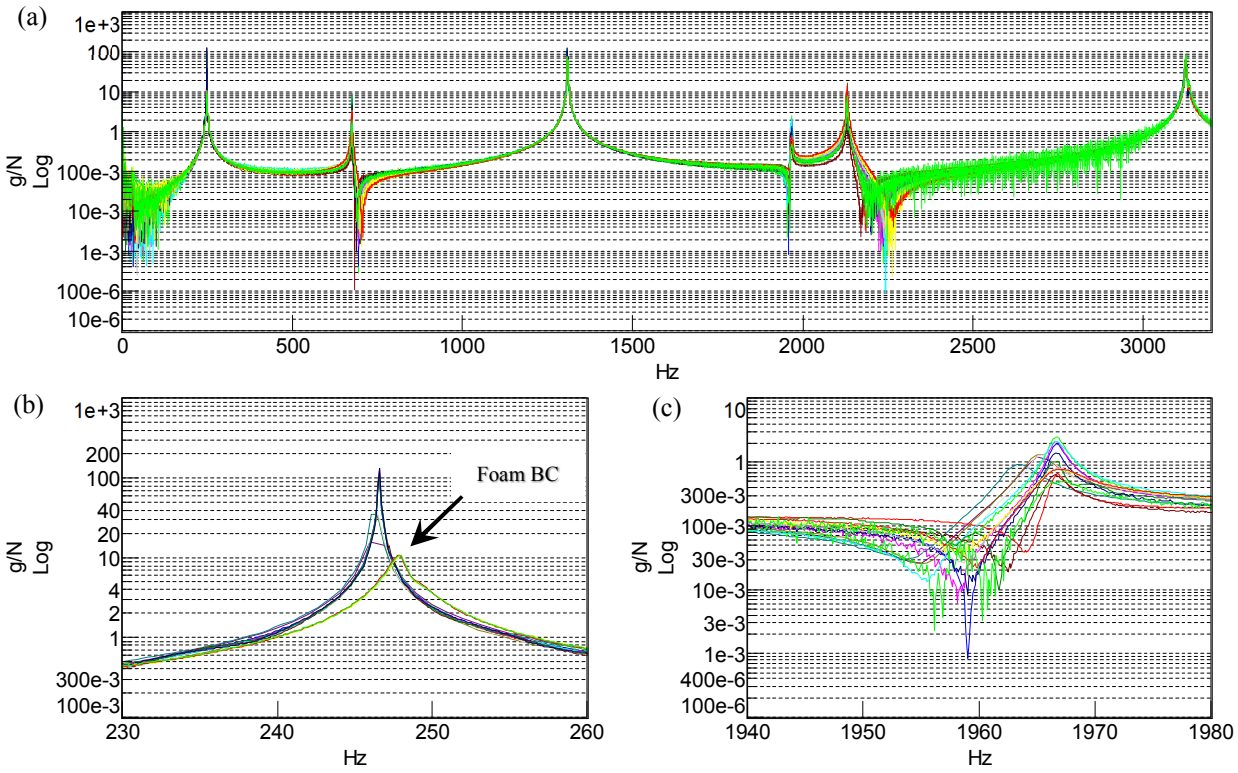

Figure 7: The FRFs of the alternative support materials for (a) the entire frequency range, (b) the first bending, and (c) first torsional mode.

The responses show that the hybrid support and fishing line support have lower damping than those seen in Test 3, displayed for comparison purposes. This indicates that the hybrid support and fishing line support do not constrain the first torsional mode as much as the bungees directly touching the specimen did. The foam, however, constrains the bending modes, which is not a desirable outcome from a support that is intended to emulate a free boundary condition. The bungee cords and foam constrain the torsional and/or translational motion of the beam, similarly to the pipe collar in [18], and needed to be considered in the system models.

2.1.3 Instrumentation

The third set of experiments consider the effects of the accelerometer attachment technique (glued versus waxed), and cable orientation. The results of attaching via glue or wax and the size of the accelerometer are shown in Figure 8. As can be seen the accelerometer attachment technique do not show any effects on the response of the structure, over the frequency range of interest; however, increasing the size of the accelerometer does affect the response. The attachment technique was expected to be the same up to about 4kHz (from discussion with someone in the field for over 30 years), and only after that wax would not be able to keep up the with response of the structure.

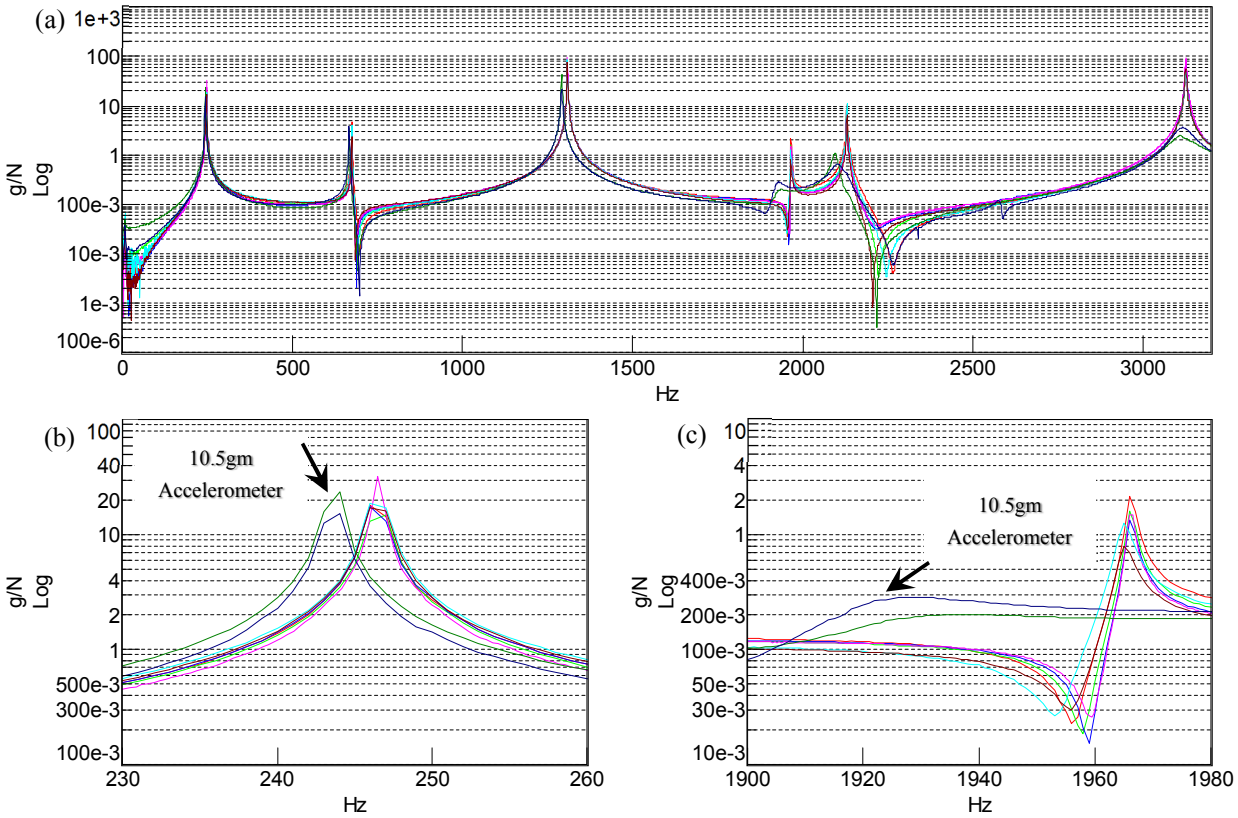

Figure 8: The FRFs of attachment technique and sensor size testing for (a) the entire frequency range, (b) the first bending, and (c) first torsional mode.

The cable orientations (hanging, supported out the side, or straight down) are shown in Figure 9, with the results shown in Figure 10. The largest shift occurs with the cables down with the hardest impact which shifts the damping from 0.05% to 0.15%; this shift could be from the way the cables are loading the beam resulting in the cables adding more damping when they hang unsupported. The cable orientation has a negligible effect on the response of the system, such that any shift could be attributed to human error for not hitting exactly the same spot.

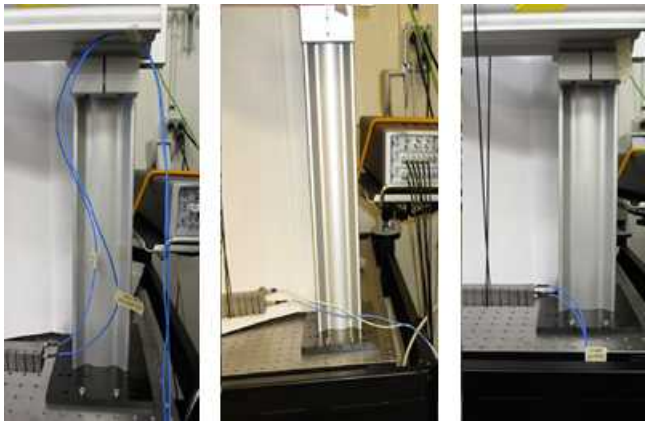

Figure 9: Sensor cable positions: (a) supported above, (b) supported across, and (c) unsupported.

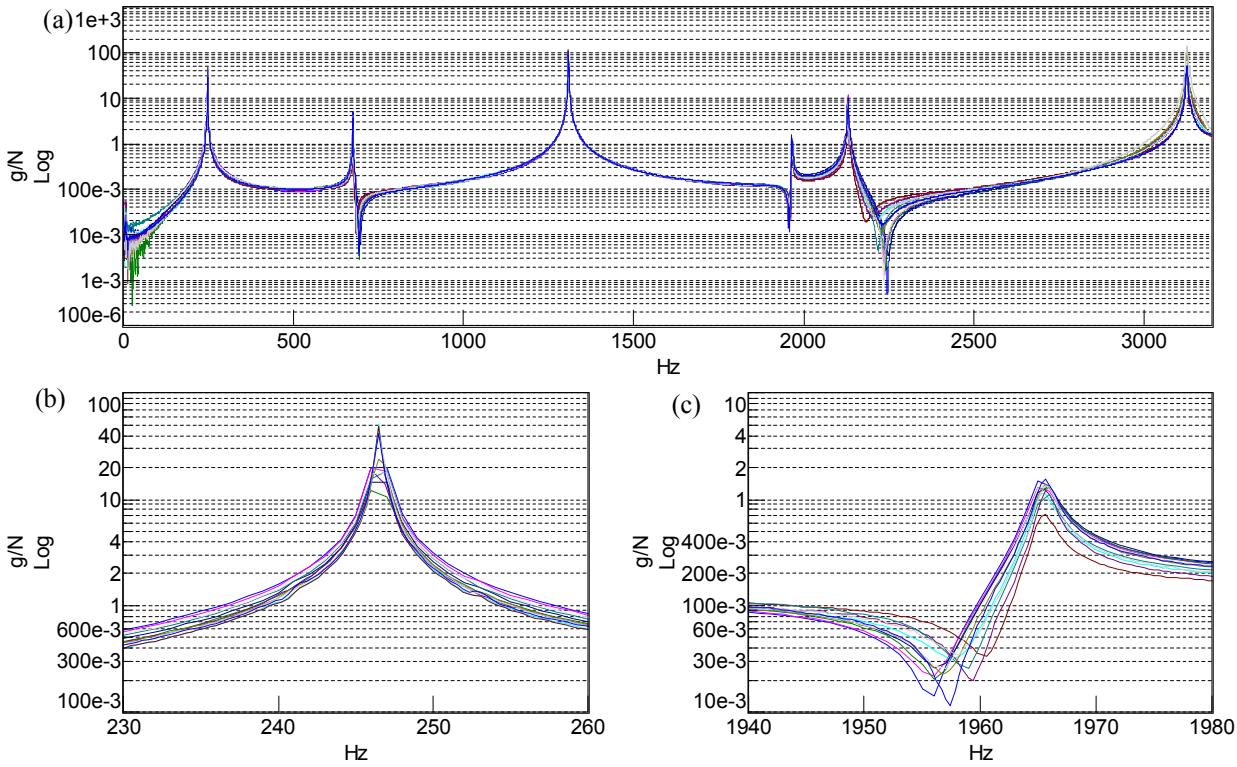

Figure 10: The FRFs of the cable orientation testing for (a) the entire frequency range, (b) the first bending, and (c) first torsional mode.

The second set of instrumentation experiments studied the effects of the number of sensors attached to the specimen. The general rule of thumb for the total mass of the sensors is less than 5% of the mass of the specimen; it is recommended by Ewins [19] to keep the mass of the sensors as small as possible. Additional sensors (with a mass of 5gm, when all are applied total approximately 0.02% of the mass of the beam) were attached to the beam as shown in Figure 11 for three additional testing scenarios, all other boundary parameters are the same as Test 3 in Table 2. The results, shown in Figure 12, show that the torsional modes of this system are influenced the most by the additional mass; the frequency for the first torsional mode shifted by 17 Hz (1%), and the damping for the second torsional mode increased from 0.05% to 0.79%.

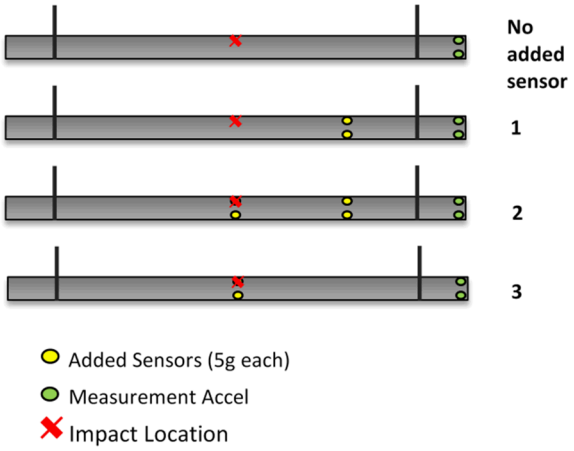

Figure 11: Added sensor testing scenarios.

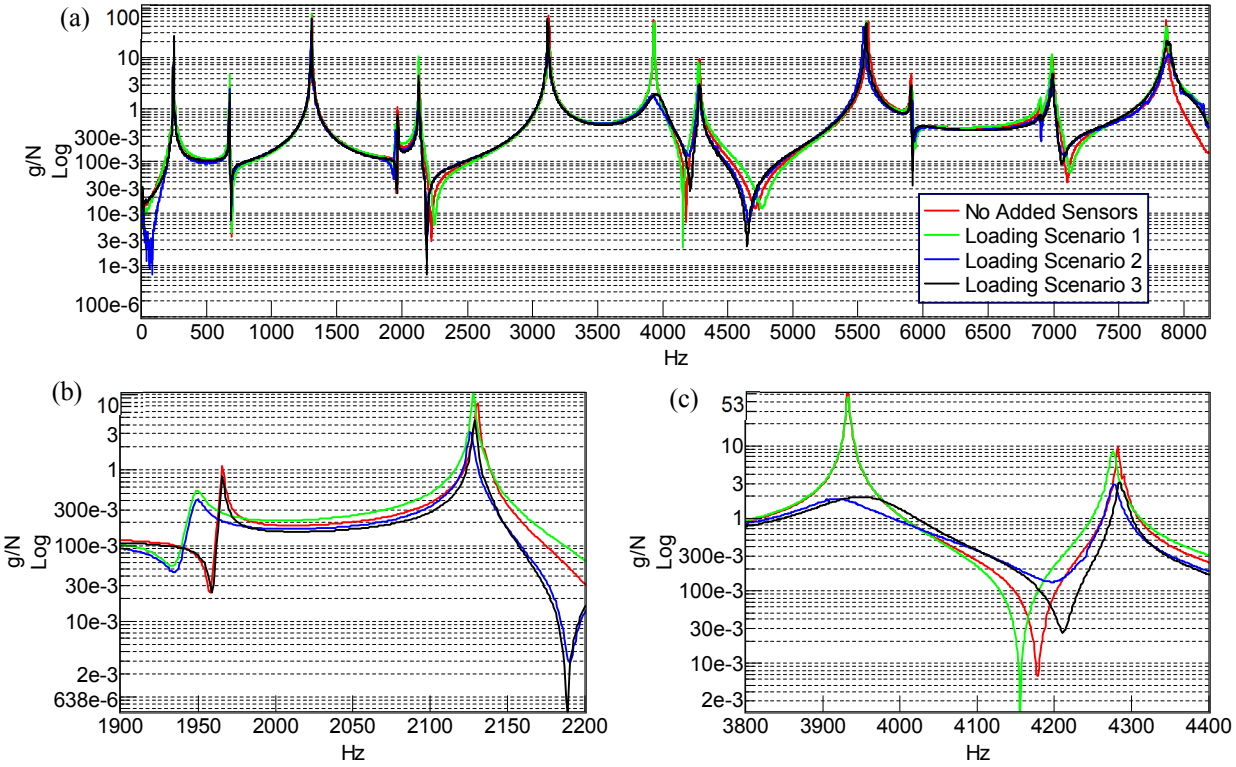

Figure 12: The FRFs of the added mass test scenarios for (a) the entire frequency range, (b) the first torsion and fourth bending, and (c) second torsion and sixth bending measured natural frequencies.

Upon closer inspection of the first torsional mode (Figure 12b) and the second torsional mode (Figure 12c), groupings of two loading scenarios appear. In Figure 12b the reference and Scenario 3 responses are grouped together, while in Figure 12c the reference and Scenario 1 responses are grouped together. These groupings come about from the additional sensors being placed on a node of those particular modes, resulting in them responding the same as the reference scenario. The shifts in frequency and damping may be from the sensors changing the moment of inertia of the beam at the anti-nodes of vibration. By contrast, when the sensors are placed at nodes versus anti-

nodes of the bending modes, the responses are unaffected (e.g. the peaks at 240, 670, and 1300 Hz). The sensors change the stiffness and mass effect of the beam less in the bending modes than the torsional modes. A simple finite element analysis confirms that the masses shift the frequency approximately the amount seen in the experimental results.

2.1.4 Test rig

The final study in this set looks at the influence of the test rig. This is to ensure that the specimen is isolated from all external sources other than the impact hammer (or shaker). The test rig is impacted with each change in bungee length or location at three different locations: at the center of the cross bar, at a location adjacent to the bungee cord, and at the attachment location to the table. The results of the test rig experiment are in the noise floor of the accelerometers; which indicates that any excitation from an outside source other than those wanted, may not be transferred to the specimen from the test rig.

2.1.5 Discussion

The testing of the experimental setup using an impact hammer resulted in all but additional sensors having little effect on the response of the system. The additional sensors significantly influenced the test beam via mass and moment of inertia changes; in the next subsection, a Polytec OFV-552 Fiber-optic Interferometer (LDV) will be tested. If using the results from an experiment with multiple sensors for model validation, all sensors should be included in computational models to match the response of the system more accurately. Testing the support structure is important, because there is potential for a shaker to excite the support structure, which would then be transferred to the bungees. The test performed by hitting the structure near the support structure indicates that the structure gave enough isolation from all but the desired inputs. The severities of the nonlinear effects from all impact hammer tests are listed in Table 3.

Table 3: Severity of the nonlinear influence from different experimental setups on the natural frequency and modal damping of the beam.

Category		Effects on Frequency	Effects on Damping	Notes
Hammer	Metal Tip	REF	REF	Frequency range with good coherence: 0-8 kHz
	White Plastic Tip	Low	Low	Frequency range with good coherence: 0-3.2 kHz
	Metal tip with added mass (75 gm)	Low	Low	More energy input into structure as low frequencies
Bungees	Full length (0.318 m)	REF	REF	
	Half length	Low	Low	Marginal frequency shifts (~1 Hz)
	Position: Inside	REF	REF	
	Position: Outside	Low	Low	Marginal frequency shifts (~1 Hz)
Boundary Material	Bungees	REF	REF	
	Fishing Line	Low	Low	Marinal frequency shift (<1 Hz) and completely constrains vertical motion
	Bungee-fishing Hybrid	Low	Low	Marinal frequency shift (<1 Hz)
	Foam	Moderate	Moderate	Frequency shift of ~4 Hz Damping increase ~367%

Sensor Size	1 gm	REF	REF	
	10.5 gm	Low	Low	The increased size results in atleast a 2 Hz frequency shift
Accelerometer	2 accelerometers glued	REF	REF	Accelerometers glued at one end of beam, each ~1 gm
	2 accelerometers attached via wax	Low	Low	Marginal frequency shifts (~1 Hz)
	Number of sensors: Scenario 1	Moderate	Moderate	Moderate change in frequency and damping
	Number of sensors: Scenario 2	High	High	Frequency shifts from ~1 Hz to ~30 Hz down (mode dependent); torsional & higher bending modes highly damped
	Number of sensors: Scenario 3	High	High	The frequency shifted up for the 2nd torsional but down for higher
	Cable orientation: above, across, unsupported	Low	Low	Cable down causes slightly higher damping for some modes (+0.1%)
Test rig		None	None	Impacts on different spots of the test rig & table

2.2 Experimental Setup Excited by Shaker

The next series of experiments utilize a shaker to study the effects of stinger type, signal type, sweep direction, and the use of a LDV compared to accelerometer measurements. The shaker is attached to the monolithic beam via a stinger connected to a PCB 208A03 force transducer at one-third the length of the beam from the edge. The type of stinger is tested to determine which of the three stingers, shown in Figure 13, has the smallest deviation from measured FRFs using the impact hammer. The results of the stinger tests using a swept sine signal are shown in Figure 14.

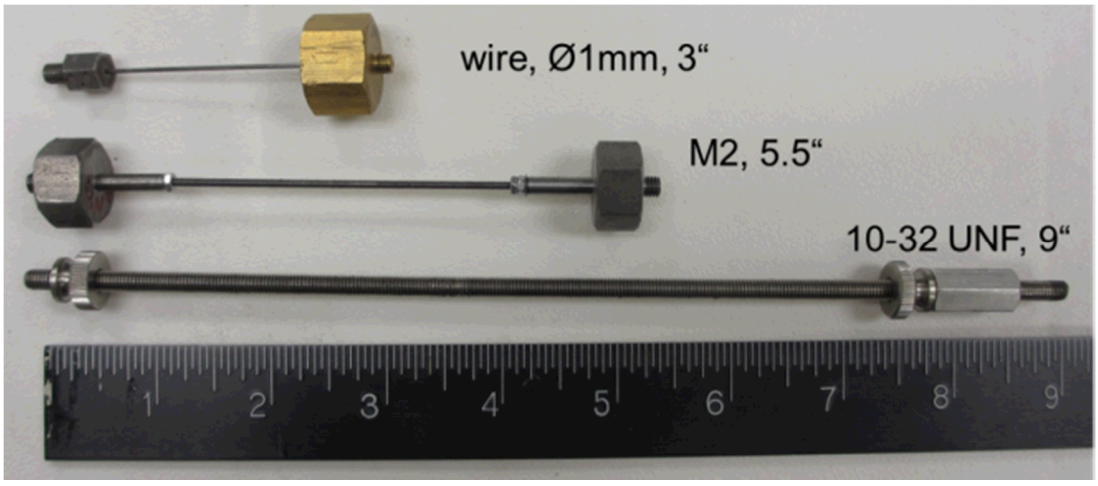

Figure 13: The three stingers tested for nonlinear effects.

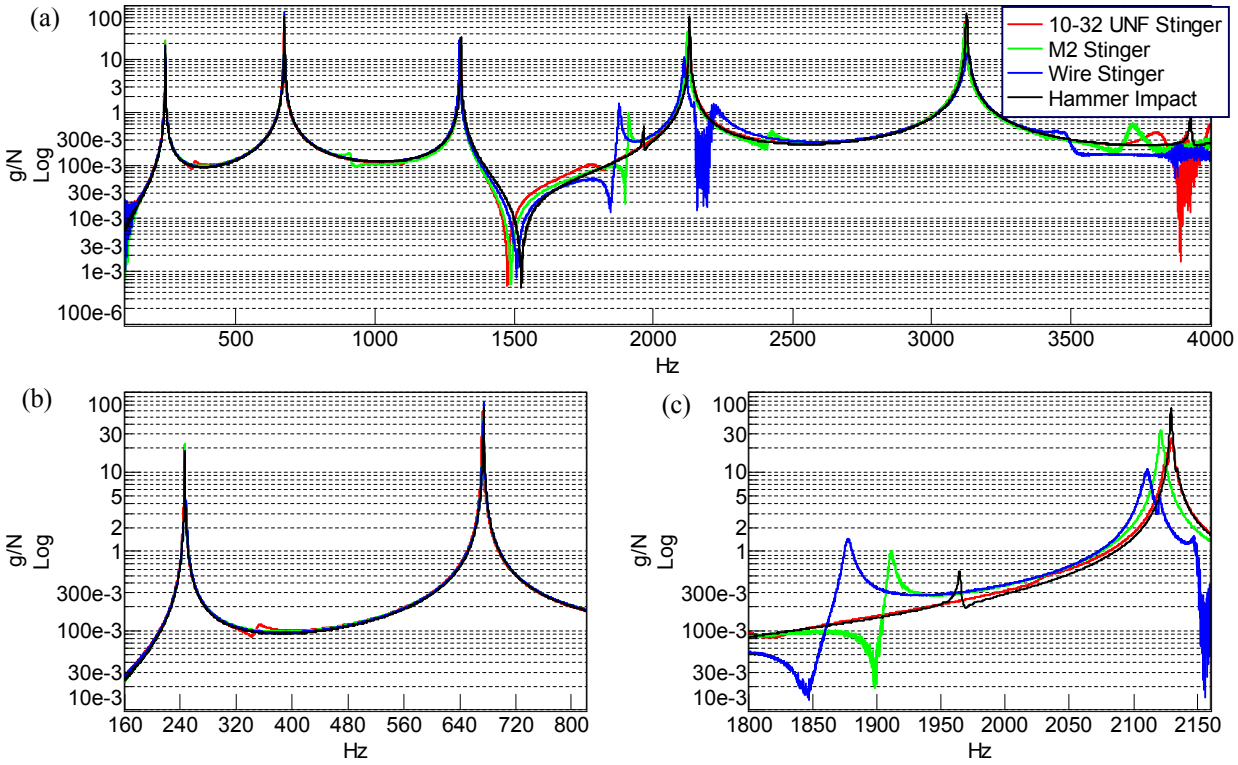

Figure 14: The FRFs of the stinger tests and one impact test for (a) the entire frequency range, (b) the first and second bending modes, and (c) the first torsional and fourth bending modes.

From the test it is seen that the wire and M2 stingers have a significant influence on the response; these stingers excite the torsional mode, which should not have been excited as the attachment location is along the center line of the beam. The excitation of the torsional modes indicates that these stingers are bending, which causes energy to be inputted into the modes; this bending could be from the force levels used or the shaker and beam not being perfectly aligned. The 10-32 UNF stinger is used in all subsequent shaker experiments. The use of the 10-32 stinger is contradictory to experience by researchers and the recommendations by Ewins [19]. A thin stinger is desired to decouple the shaker from the specimen motion not in the direction of excitation; thus, removing the bending moment applied at the force transducer [20]. However, the stingers available during the testing are much longer than recommended [19]; resulting in the larger diameter being a better choice for this experiment.

The final experiments on the monolithic beam test the sweep direction and speed, the signal type, and the use of an LDV; the results of these tests are shown in Figure 15. The results show that the white noise should not be used as the torsional modes are excited, which could be from the stinger modes being excited more with white noise than a sweep signal. The LDV has a significant frequency shift that can be associated with the sensors being removed from the beam. The severity of the nonlinear effects from the various shaker setup tests are listed in Table 4.

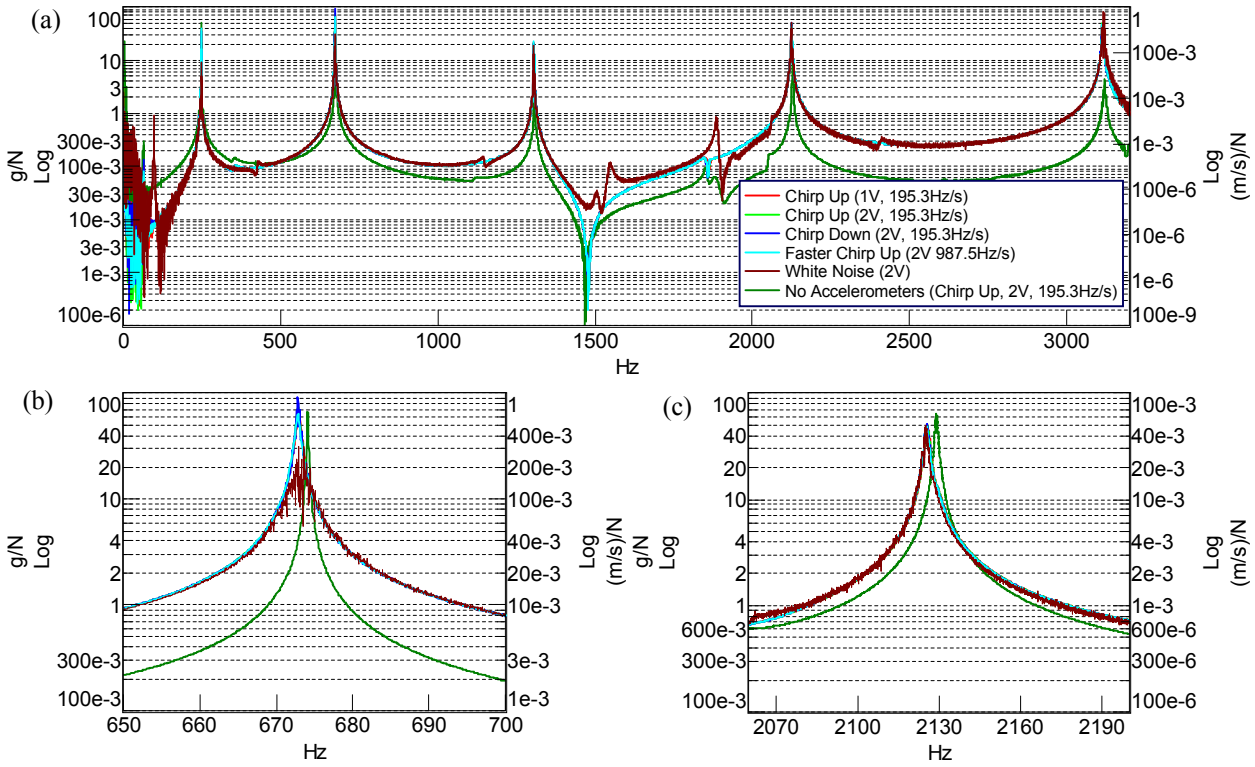

Figure 15: The FRFs of the shaker signal tests over (a) the entire frequency range, (b) near the second bending mode, and (c) near the fourth bending mode.

Table 4: Severity of the nonlinear influence of shaker test setups on frequency and damping of the beam

Category		Effects on Frequency	Effects on Damping	Notes
Stingers	None	REF	REF	Impact hammer test
	10-32 UNF (9in)	Low	Low	No torsional modes excited, matches best to hammer tests
	M2 (5.5in)	Moderate	None	Frequency shift down
	Wire (3in)	Moderate	None	Frequency shift down, torsional modes excited, stinger bending occurs
Excitation Amplitude (V)	Nominal	REF	REF	2V amplitude
	(1V)	None	Low	Marginal frequency shift ~1 Hz
Signals	Chirp Up	REF	REF	Swept at 195.3Hz/s
	Chirp Down	None	Low	Linear structure tested
	Sweep Rate (987.5Hz/s)	None	None	No visable influence
	White noise	Low	None	Noisy FRFs; anti-resonances observed
Accelerometer	Two accelerometers	REF	REF	Accelerometers Glued on
	No acclerometers (LDV)	Moderate	Low	Frequency shifts to slightly higher frequencies

2.3 Effects of Boundary Condition Type

A "fixed-free" boundary is difficult to achieve using clamps [7]. To try and create a "fixed" boundary, a method that can be used is to epoxy the specimen to a larger-stiffer structure. Here,

one end of a half-beam is epoxied to a 0.127m x 0.127m x 0.1524m, 20kg steel block, which is then clamped to the table (Figure 16). The boundary is then tested by attaching a shaker to the beam using an off-center hole located one-third the length of the beam in from the free end.

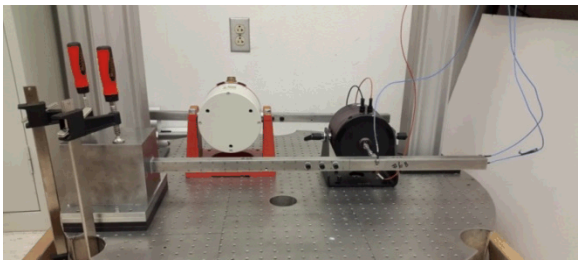

Figure 16: Experimental setup for the "fixed-free" boundary test.

The rigidness of the "fixed" boundary is tested, utilizing a stepped-sine signal, ranging from 584.5 Hz to 585.5 Hz (around the second bending). To investigate the relative displacement in the joint, two accelerometers (PCB 354A01) are attached to the beam and block, near the interface, as shown in Figure 17. The amplitude of response on the beam and block are measured for 5 g and 15 g acceleration input control. The acceleration of the beam is compared to that of the block, shown in Figure 18. The results of this study indicate that the boundary is not truly fixed, but closer to that of a pinned joint with translational and rotational springs. A truly fixed boundary would be a point at the origin or a small vertical line, because there should be no motion in the boundary or on the beam at the boundary. Thus, together with [7], [21] and [22], it is evident that extraordinary lengths are needed to achieve a fixed boundary condition, created using epoxy or clamping the beam; and these conditions should be avoided if possible.

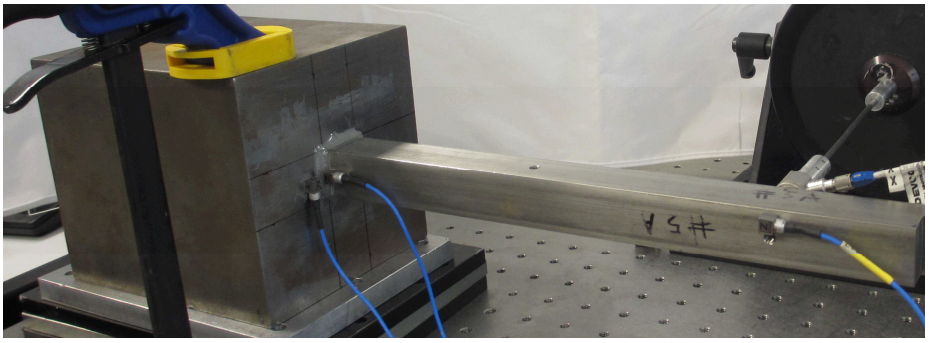

Figure 17: Locations of the accelerometers for testing the rigidness of the "fixed" boundary, the yellow star is the location on block, and red the location on the beam.

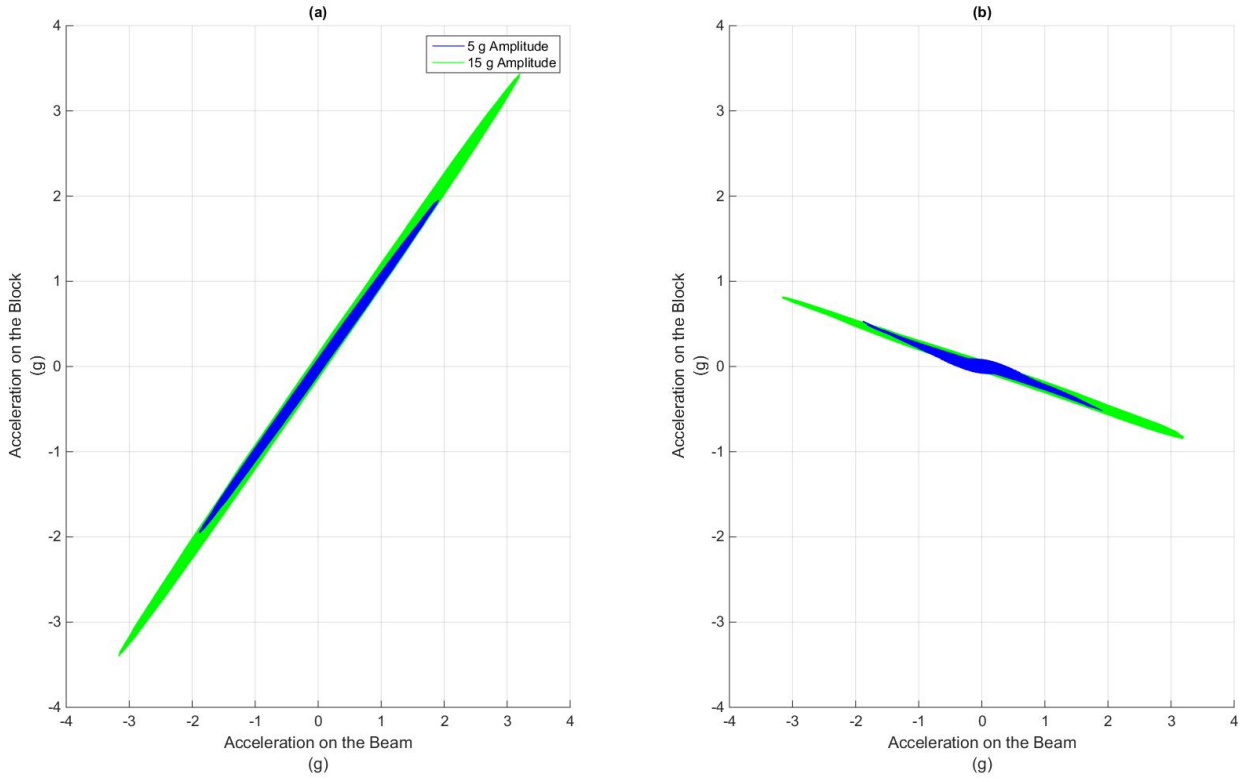

Figure 18: Acceleration on the beam in the vs. acceleration on the block with (a) sensor direction parallel and (b) perpendicular, to test the rigidness of the "fixed" boundary.

3 Effects of Control Parameters

The nonlinearities in a jointed beam are difficult to identify due to part-to-part and experiment-to-experiment variability associated with the interfacial conditions [10] (including distribution of asperities, grain boundaries, dislocation surfaces, other microstructure related quantities, and global geometry of effects, e.g. curved interfaces). To measure the effects of the nonlinearity, the amplitude of excitation or input force needs to be held constant. Whether the amplitude or force are held constant, is dependent on:

1) If the effects of force-drop-out at resonance will distort the measured response due to the measurement of noise [23]
2) If using linear assumptions to extract the data as the damping and stiffness of nonlinear systems can be amplitude dependent [23]
3) Comparing to numerical models; most are based on constant force as constant amplitude cause numerical computation errors [16].

To test a control algorithm, a jointed beam with the "free-free" boundary conditions is implemented. The "free-free" condition is implemented two different ways; the first is the same as those presented in the previous section (Figure 2), and the second is by using 1.2m of 50lb fishing line.

An open loop control algorithm can possibly have five parameters that affect the measurement of a transfer function (TF). The first parameter is the confidence in measured system FRF, which

dictates whether the algorithm can deviate from the measured system FRF (received from a low level white noise test). The next parameter is the proportional gain, which specifies the amount the algorithm corrects divergence from the control level in one step. The third parameter is the number of delay cycles; this parameter specifies how long to wait for steady state to be reached before taking a measurement. The fourth parameter is the number of hold cycles (NHCs); this parameter is how many periods the algorithm measures the response of the system. The last parameter is the step size, which controls the frequency resolution of the TF.

The control algorithm tested is LMS Test.Lab 15A MIMO Sweep & Stepped Sine, which is a linear control algorithm (it does not control higher harmonics, such as in [24]). The control parameters tested are listed in Table 5, with the default parameters in Test.Lab listed (Note: Proportion Gain is named Error Correction Factor (ECF) in Test.Lab), as well as how the parameters are tested. The last column ("optimal") is discussed later in the section. The default parameters are tested using the bungee "free-free" BRB under 1.75N force control, the results are shown for various torque levels; this is used as an example of the response from the default parameters. As can be seen in Figure 19, the default parameters do not produce a smooth TF, which is what is expected when using a control algorithm.

Table 5: Control parameters used in control study.

Control Parameters	Default	Test	Optimal
Confidence in Measured System FRF	High	Low	Low
Error Correction Factor	100%	Vary	60%
Number of Delay Cycles	1	30	30
Number of Hold Cycles	15	Vary	40
Step Size	0.1Hz	0.05Hz	0.05Hz

(a)

(b)

(c)

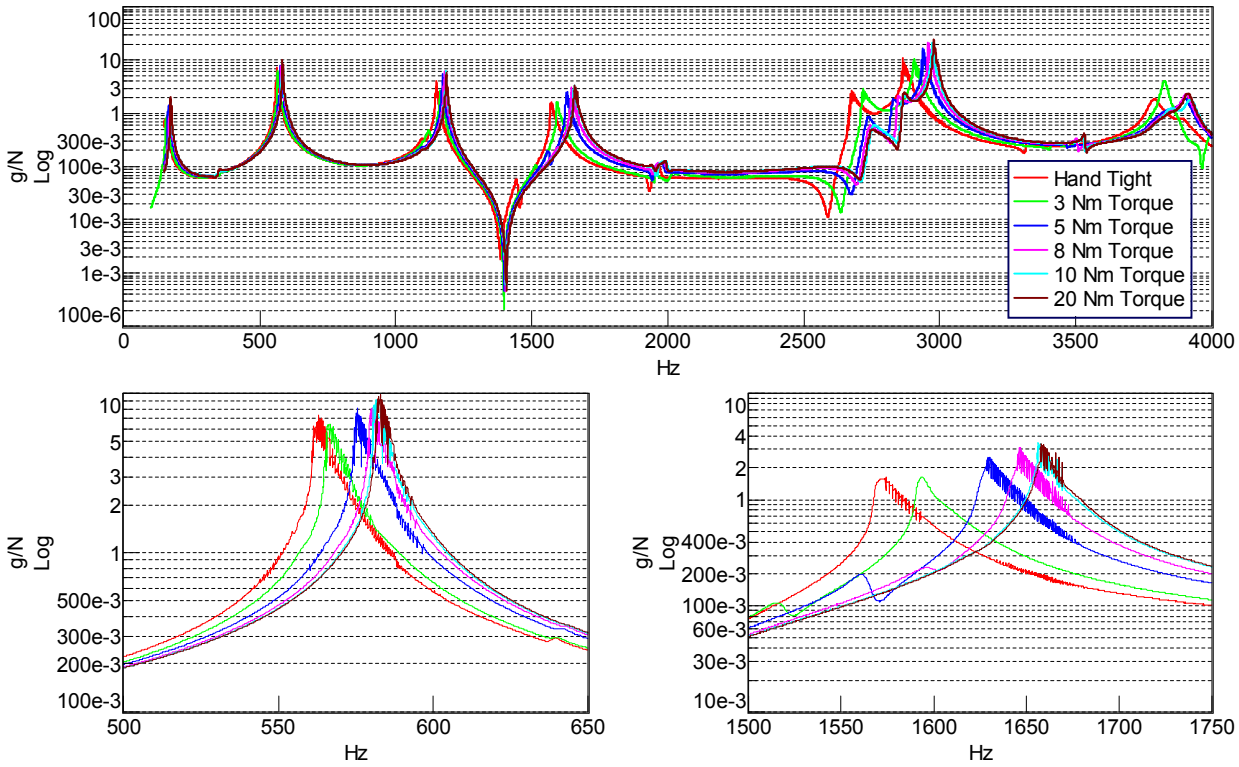

Figure 19: The TFs of the default control parameters for (a) the entire frequency range, (b) the second bending mode, and (c) the fourth bending mode.

Further investigation into how the control algorithm works, indicated that the confidence in measured system FRF, number of delay cycles, and step size should be set to Low confidence, 30 cycles, and 0.05Hz, respectively, for best performance when exciting a nonlinear system. The ECF and NHC are then tested for how they affect the response TFs. The measurements are performed on the "free-free" (fishing line) boundary condition BRB, with a 10Nm torque applied to the bolts.

Different values of the ECF are compared in the frequency ranges of 570-580Hz (second bending) and 1176-1184Hz (third bending), with 40 hold cycles, and a 5N input force level or 10g amplitude input level. The results, shown in Figure 20 and Figure 21, compare the measurements for stepping up (top row) or stepping down (bottom row) through the defined frequency ranges.

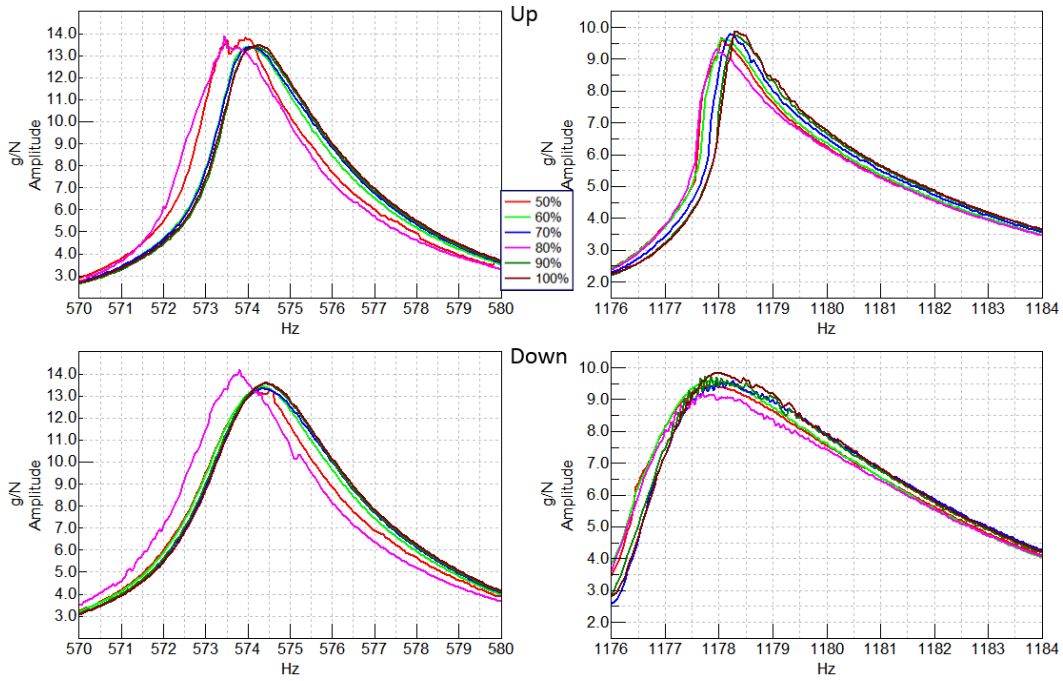

Figure 20: TFs of 5N force control to locate optimal ECF; (top row) sweep up, (bottom row) sweep down, (left column) second bending mode, and (right column) third bending modes.

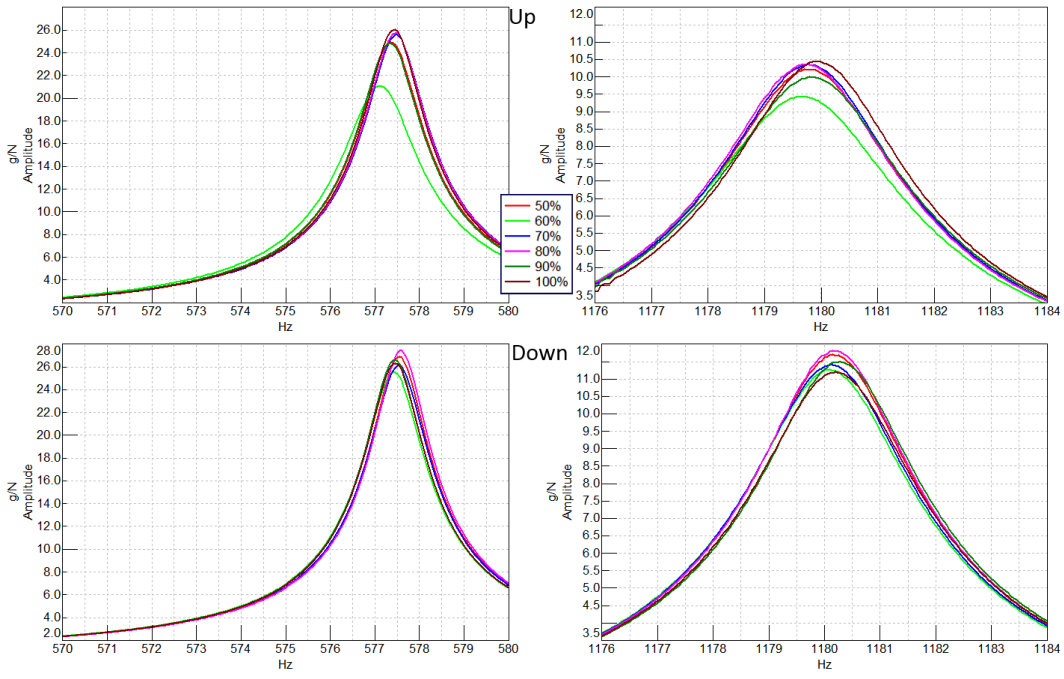

Figure 21: TFs of 10g acceleration control to locate optimal ECF; (top row) sweep up, (bottom row) sweep down, (left column) second bending mode, and (right column) third bending modes.

An ECF of 60% is the best balance of speed and accuracy for the control algorithm for most input control types. When the value is set higher than 60% the TF exhibits a sawtooth-like look in

the default parameter test; while values below 60% did not correct errors, when the levels are inside the control bands or corrected slowly back to the desired levels.

The NHCs are then tested after the optimal EFC is determined, shown in Figure 22 and Figure 23 for force and amplitude control, respectively. As shown in Figure 22 and Figure 23, 40 and 60 NHCs result in the smoothest TFs. The optimal NHCs is set to 40 cycles, because 60 cycles result in the experimental time to be nearly double that of 40. The optimal parameters for this system are listed in Table 5.

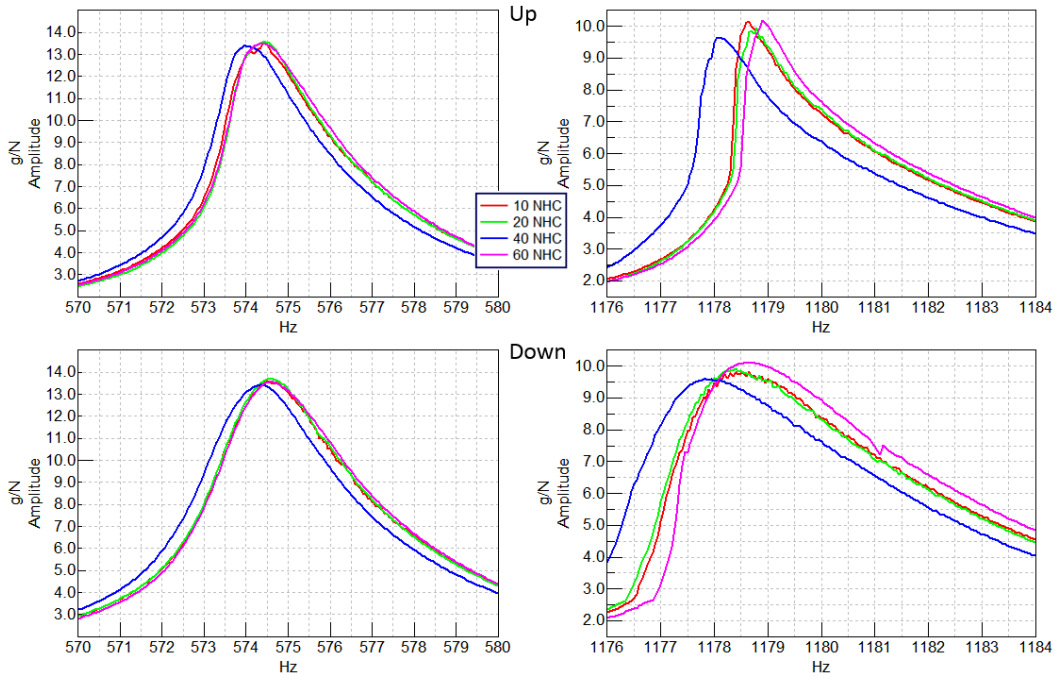

Figure 22: TFs of 5N force control to locate optimal NHC; (top row) sweep up, (bottom row) sweep down, (left column) second bending, and (right column) third bending modes.

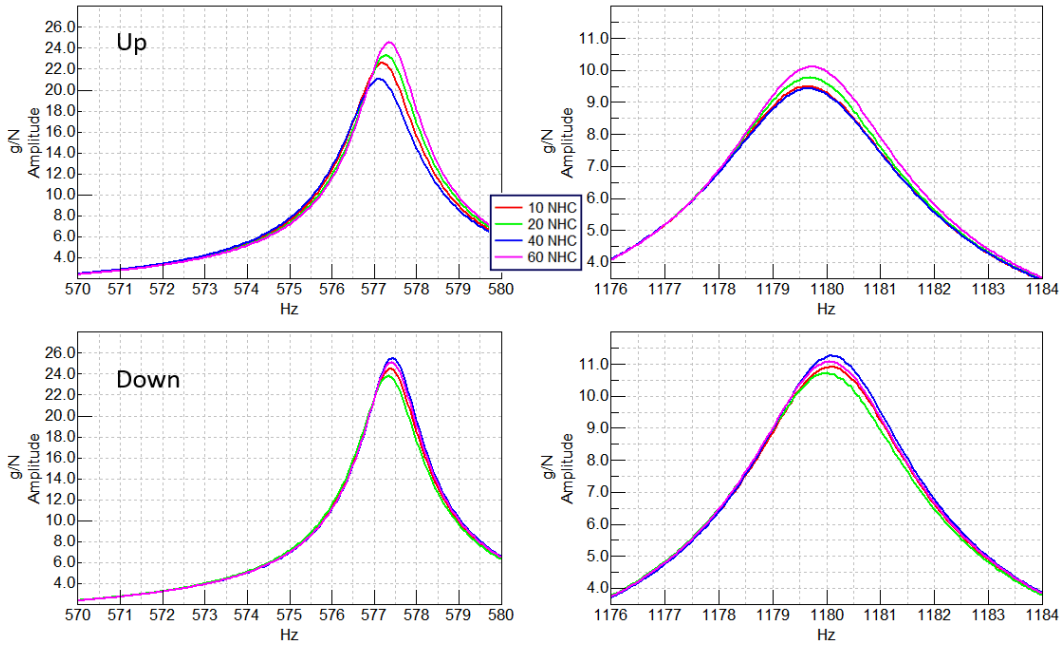

Figure 23: TFs of 10g acceleration control to locate optimal NHC; (top row) sweep up, (bottom row) sweep down, (left column) second bending, and (right column) third bending mode.

Figures Figure 20 through Figure 23 show that the longer the signal is held the smoother the response in the frequency domain will be, this is because the response reaches the steady state response of the system fully. The correction factor value also drives the smoothness of the frequency response because if the input deviates to far this will drive how much the system will be corrected in one step. The lower ECFs do not correct deviation from the control level as fast if at all, and the higher ECFs over correct and cause a jump in the response.

The figures also show that the saw tooth effect is seen in force control more than acceleration amplitude control. The source of this could come from the force level dropping drastically at resonance, requiring the controller to output more voltage quickly in order to maintain the same force level. The increase in voltage also dictates that the force level cannot be set high as the shaker can only handle up to a certain level of amperage. Acceleration control does not have as great of an effect because the opposite happens, as long as the range of interest does not have anti-resonances which have the same effect as force on resonance: as the acceleration increases, the voltage needs to decrease, which is easier and less restrictive. It is recommend to use acceleration control, which is similar to the method in [23], if the shaker being used cannot handle the desired force levels.

The optimal parameters and default parameters are compared using a 10g acceleration amplitude control, shown in Figure 24. The TF comparison (Figure 24a) shows that the optimal parameters have removed the saw tooth effect from the default parameters. The amount of time for the test (Figure 24b & c) does increase; however, the acceleration was controlled to the level specified. Thus, even for a system with a strong nonlinearity, such as the BRB, it is possible to

find control parameters that allow for the measurement of a smooth TF. Responses that contain sawtooth-like features should therefore be rejected until optimal control parameters can be found.

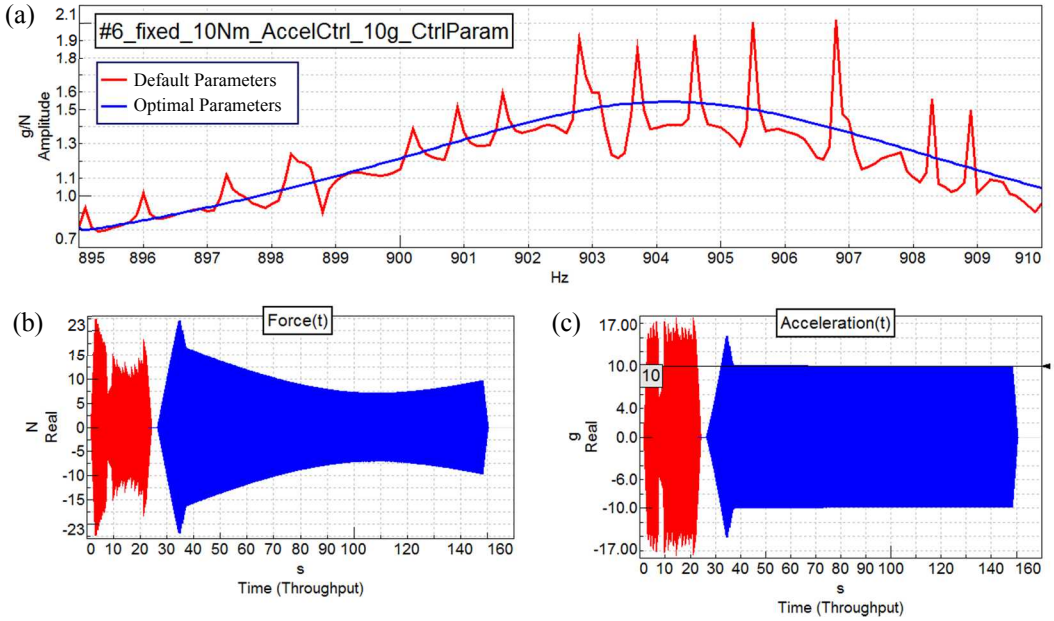

Figure 24: Comparison of the (a) TF and time signals using (red) the default parameters and (blue) optimal parameters of the (b) force and (c) acceleration.

4 Conclusions

This work sought to identify a set of recommendations for conducting experiments on nonlinear systems using conventional measurement techniques. The effects of the test setup (boundary conditions, excitation techniques, and measurement techniques) are studied to understand the effect on the system's stiffness and damping. This research highlights that it is important to think of the experimental system as the entire test setup, not just the test specimen. Changes to this system are shown to have varying effects. Specific recommendations are:

- Impact hammer measurements: the tip and hammer mass do not significantly affect the measurements of damping and stiffness over the frequency range of interest. Therefore, the hammer configuration should be such that the bandwidth of interest is excited.
- Boundary Conditions: the response of the system is insensitive to: the length, stiffness, and position of bungee cables used for making the "free" boundary condition. The bungee setup should be such that the rigid body modes are much less than the first elastic mode of the test specimen.
- Boundary Conditions: the use of fishing line is desirable as the torsional modes of the specimen are less constrained. However, a pure boundary of fishing line is not recommended, as the vertical motion of the specimen is constrained in the downward direction.

- Boundary Conditions: the use of foam is not recommended as it constrains bending and torsional modes at the same time. Due to the material, foam also adds damping into the system and needs to be accounted for when analyzing the response of the specimen.
- Boundary Conditions: if a "fixed-free" boundary is desired, any model being compared needs to include the stiffness of the attachment technique, and recognize that this is an additional joint with its own nonlinear effects.
- Accelerometers: even when the mass of the accelerometers is less than 0.02% of the structure's, they need to be included in models. When used, accelerometers should be located away from nodes, included in modeling, and kept to the minimum necessary.
- Shaker measurements: care should be taken when selecting a stinger for shaker tests, because the force level required to drive and identify the nonlinearity may cause the stinger to bend. A thinner stinger may be the most desired stinger due to low mass effect and reduced coupling between the specimen and shaker; however, the thinner the stinger the lower the stiffness, which results in stinger modes bleeding into the response of the structure.

Control parameters are tested and recommendations for the optimal parameters are:

- The system FRF measured with white noise should not be considered an accurate representation of the system.
- The proportional gain should be set such that the control algorithm does not completely correct for a deviation in one step.
- A sufficient number of delay cycles should be used such that steady state is reached after each step, more delay cycles maybe needed for nonlinear systems with greater damping than a linear system.
- A Convergence study on the number of hold cycles should be conducted to ensure that the steady state response can be fully measured.

It is also recommended that acceleration amplitude control be used instead of force control; however, care must be taken in using the results as the response may jump between different response curves.

ACKNOWLEGDEMENTS

The authors would like to thank Dr. Matthew Allen (University of Wisconsin-Madison), William Flynn (Siemens), Juan Carlos Bilbao-Ludena (Technical University of Berlin), Florian Morlock (University of Stuttgart), Benjamin Pacini (Sandia National Laboratories), and Randall Mayes (Sandia National Laboratories) for their input during the tests.

Funding

This work was conducted at the Nonlinear Mechanics and Dynamics (NOMAD) research institute host by Sandia National Laboratories during the summers of 2014 and 2015. Sandia National Laboratories is a multi-mission laboratory managed and operated by Sandia Corporation,

a wholly owned subsidiary of Lockheed Martin Corporation, for the U.S. Department of Energy's National Nuclear Security Administration under contract DE-AC04-94AL85000.

5 References

[1] D. J. Inman, Engineering Vibration, 4 ed., Upper Saddle River: Pearson, 2014.

[2] J. P. Noël and G. Kerschen, "Frequency-domain subspace identification for nonlinear mechanical systems," *Mechanical Systems and Signal Processing,* vol. 40, pp. 701-717, 2013.

[3] M. W. Sracic, M. S. Allen and H. Sumali, "Identifying the modal properties of nonlinear structures using measured free response time histories from a scanning laser Doppler vibrometer," in *IMAC XXX A Conference and Expostions on Structural Dynamics*, Jacksonville, FL, 2012.

[4] M. R. Brake, "The Role of Epistemic Uncertainty of Contact Models in the Design and Optimization of Mechanical Systems with Aleatoric Uncertainty," *Nonlinear Dynamics,* vol. 77, pp. 899-922, 2014.

[5] M. R. Brake, "The Effect of the Contact Model on the Impact-Vibration Response of Continuous and Discrete Systems," *Journal of Sound and Vibrations,* vol. 332, pp. 3849-3878, 2013.

[6] R. J. Kuether, M. R. Brake and M. S. Allen, "Evaluating Convergence of Reduced Models Using Nonlinear Normal Modes," in *IMAC XXXII A Conference and Exposition on Structural Dynamics*, Orlando, FL, 2014.

[7] C. W. Schwingshackl, C. Joannin, L. Pesaresi, J. S. Green and N. Hoffmann, "Test Method Development for Nonlinear Damping Extraction of Dovetail Joints," in *IMAC XXXII A Conference and Exposition on Structural Dynamics*, Orlando, FL, 2014.

[8] D. J. Segalman, D. L. Gregory, M. J. Starr, B. R. Resor, M. D. Jew, J. P. Lauffer and N. M. Ames, Handbook on Dynamics of Jointed Structures, Albuquerque, NM: SAND2009-4164, Sandia National Laboratories, 2009.

[9] W. Heisenberg, Physics and Philosophy: The Revolution in Modern Science, London: George Allend and Unwin LTD, 1959.

[10] M. R. Brake, P. Reuß, D. J. Segalman and L. Gaul, "Measurements and Modeling of Variability and Repeatability of Jointed Structures with Frictional Interfaces," in *IMAC XXXII A Conference and Exposition on Structural Dynamics*, Orlando, FL, 2014.

[11] P. Reuss, S. Kruse, S. Peter, F. Morlock and L. Gaul, "Identification of Nonlinear Joint Characteristic in Dynamic Substructuring," in *Topics in Experimental Dynamic Substructuring: Proceedings of the 31st IMAC, A Conference on Structural Dynamics*, vol. 2, R. L. Mayes, D. J. Rixen and M. Allen, Eds., New York, Springer, 2013, pp. 27-36.

[12] K. Worden and G. Tomlinson, Nonlinearity in Structural Dynamics: Detection, Identification and Modelling, Philadelphia: Institute of Physics Publishing, 2001.

[13] B. J. Deaner, M. S. Allen, M. J. Starr, D. J. Segalman and H. Sumali, "Application of Viscous and Iwan Modal Damping Models to Experimental Measurements from Bolted Structures," *Journal of Vibration and Acoustice,* vol. 137, pp. 021012-1 -- 021012-12, 2015.

[14] T. G. Carne, D. T. Griffith and M. E. Casias, "Support conditions for experimental modal anaylsis," *Journal of Sound and Vibrations,* vol. 41, no. 6, pp. 10-16, 2007.

[15] H. Herlufsen, "Application Note: Modal Analysis using Multi-reference and Multiple-Input Multiple-Output Techniques," Brüel & Kjær, Denmark, 2012.

[16] R. M. Lacayo, L. Pesaresi, D. Fochler, J. Groß, M. R. Brake and C. W. Schwingshackl, "A Numerical Round Robin to Predict the Dynamics of an Experimentally-Measured Brake-Reuss Beam," in *IMAC XXXV A Conference and Exposition on Structural Dynamics*, Garden Grove, CA, 2017.

[17] M. R. Ashory, High Quality Modal Testing Methods, London, UK: Doctoral Thesis, Imperial College of Science, Technology and Medicine London, 1999.

[18] B. Zhang, T. P. Waters and B. R. Mace, "Identifying joints from measured reflection coefficients in beam-like structures with application to a pipe support," *Mechanical Systems and Signal Processing,* vol. 24, no. 3, pp. 784-795, 2010.

[19] D. J. Ewins, Modal Testing: theory, practice, and application, 2 ed., Philadelphia, PA: Research Studies Press LTD, 2000.

[20] M. J. Ratcliffe and N. A. Lieven, "A GENERIC ELEMENT-BASED METHOD FOR JOINT IDENTIFICATION," *Mechanicical Systems and Signal Processing,* vol. 14, no. 1, pp. 3-28, 2000.

[21] Ş. Tol and H. N. O¨zgu¨ven, "Dynamic characterization of bolted joints using FRF decoupling and optimization," *Mechaincal Systems and Signal Processing,* Vols. 54-55, pp. 124-138, 2015.

[22] Z.-C. Wang, Y. Xin and W.-X. Ren, "Nonlinear structural joint model updating based on instantaneous characteristics of dynamic responses," *Mechanical Systems and Signal Processing,* Vols. 76-77, pp. 476-496, 2016.

[23] A. Carrella and D. Ewins, "Identifying and quantifying structural nonlinearities in engineering applications from measured frequency response fuctions," *Mechanical Systems and Signal Processing,* vol. 25, no. 3, pp. 1011-1027, 2011.

[24] F. Morlock, Force Control of an Electrodynamic Shaker for Experimental Testing of Nonlinear Mechanical Structures, Master Thesis, Stuttgart: Universität Stuttgart, 2015.